Available online at www.sciencedirect.com
ScienceDirect
Journal of Hazardous Materials 157 (2008) 344–351
Journal of Hazardous Materials
www.elsevier.com/locate/jhazmat

Equilibrium, kinetics and mechanism of malachite green adsorption on activated carbon prepared from bamboo by K_2CO_3 activation and subsequent gasification with CO_2

B.H. Hameed [a,*], M.I. El-Khaiary [b]

[a] *School of Chemical Engineering, Engineering Campus, Universiti Sains Malaysia, 14300 Nibong Tebal, Penang, Malaysia*
[b] *Chemical Engineering Department, Faculty of Engineering, Alexandria University, El-Hadara, Alexandria 21544, Egypt*

Received 29 September 2007; received in revised form 30 December 2007; accepted 31 December 2007
Available online 6 January 2008

Abstract

In this work, the adsorption of malachite green (MG) was studied on activated carbon prepared from bamboo by chemical activation with K_2CO_3 and physical activation with CO_2 (BAC). Adsorption studies were conducted in the range of 25–300 mg/L initial MG concentration and at temperature of 30 °C. The experimental data were analyzed by the Freundlich isotherm, the Langmuir isotherm, and the multilayer adsorption isotherm. Equilibrium data fitted well with the Langmuir model with maximum adsorption capacity of 263.58 mg/g. The rates of adsorption were found to confirm to pseudo-second-order kinetics with good correlation and the overall rate of dye uptake was found to be controlled by pore diffusion throughout the entire adsorption period. The results indicate that the BAC could be used to effectively adsorb MG from aqueous solutions.

Keywords: Activated carbon; Adsorption isotherm; Bamboo; Kinetics; Malachite green

1. Introduction

Synthetic dyestuffs are used extensively in textile, paper, printing and other industries. Dyes are classified as follows: anionic-direct, acid and reactive dyes; cationic-basic dyes; non-ionic-disperse dyes [1,2]. Basic dyes have high brilliance and intensity of colours and are highly visible even in a very low concentration [2,3–7]. It is reported that there are over 100,000 commercially available dyes with a production of over 7×10^5 metric tonnes per year [3,8]. Dyes may significantly affect photosynthetic activity in aquatic life due to reduced light penetration and may also be toxic to some aquatic life due to the presence of aromatics, metals, chlorides, etc., in them [1–4,8,9].

Malachite green selected in this study has been widely used in aquaculture as a parasiticide and in food, health, textile and other industries for one or the other purposes. It controls fungal attacks, protozoan infections and some other diseases caused by helminths on a wide variety of fish and other aquatic organisms. However, the dye has generated much concern regarding its use due to its reported toxic effects [10]. Many adverse effects from the consumption of the dye due to its carcinogenic, genotoxic, mutagenic and teratogenic properties in animal studies have been reported [11].

Various attempts have been made for dye removal from aqueous solutions. These include photodegradation [12,13], photocatalytic degradation [14,15], adsorption [16] and others [12]. Adsorption has been shown to be the most promising option for all on-biodegradable organics for the removal from aqueous streams, activated carbons being the most common adsorbent for this process due to its effectiveness and versatility. Our group have successfully prepared activated carbons using different precursors such as oil palm fibre [17], rattan sawdust [18], coconut husk [19], *Hevea brasiliensis* seed coat [20], and bamboo [21]. The bamboo-based activated carbon was previously prepared by activation with KOH and gasification with CO_2 for removal of methylene blue [21]. In this paper, we report the adsorption of malachite green on activated carbon prepared from bamboo by chemical activation with K_2CO_3 and subsequent physical activation with CO_2. K_2CO_3 is not a hazardous chemical and not deleterious as it is frequently used for food additives [22]. K_2CO_3 was used for preparation of activated carbons from palm shell [22], cork waste [23] and chickpea husk [24]. Thus, the

* Corresponding author. Tel.: +60 4 599 6422; fax: +60 4 594 1013.
E-mail address: chbassim@eng.usm.my (B.H. Hameed).

0304-3894/$ – see front matter © 2008 Elsevier B.V. All rights reserved.
doi:10.1016/j.jhazmat.2007.12.105

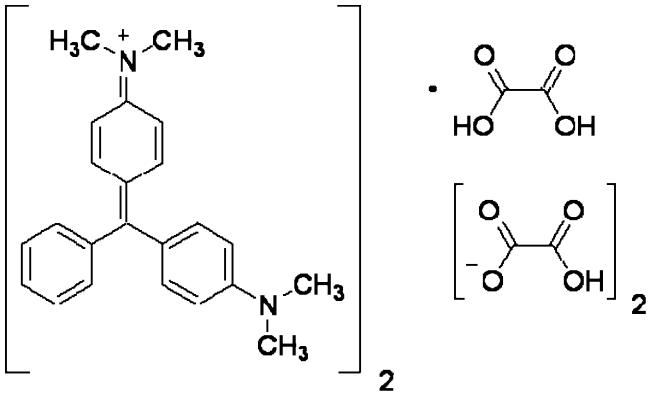

Fig. 1. Chemical structure of malachite green oxalate.

objective of the research was to evaluate the adsorption potential of activated carbon prepared from bamboo for malachite green. The kinetics of adsorption was also studied and the processes controlling the rate of mass transfer were determined.

2. Materials and methods

2.1. Adsorbate

The dye, malachite green oxalate, C.I. Basic Green 4, C.I. Classification Number 42,000, chemical formula = $C_{52}H_{54}N_4O_{12}$, MW = 927.00, λ_{max} = 618 nm (measured value) was supplied by Sigma–Aldrich (M) Sdn Bhd, Malaysia and used as received. Fig. 1 shows the chemical structure of malachite green oxalate.

2.2. Preparation and characterization of activated carbon

Raw material (bamboo) used for preparation of activated carbon was procured locally, washed, dried, and crushed to desired mesh size (1–2 mm). A certain amount of raw material was soaked with (K_2CO_3) at impregnation ratio of 1:1. The mixture was dehydrated in an oven overnight at 105 °C. The dehydrated sample was placed in a stainless steel vertical tubular reactor placed in a tube furnace under high purity nitrogen (99.995%) flow of 150 cm^3/min to a final temperature of 500 °C. The heating was provided at rate of 15 °C/min for 1 h. Then the temperature was increased to 850 °C. Once the final temperature was reached, the gas flow was switched to carbon dioxide and activation was continued for 2 h. The activated product was then cooled to room temperature under nitrogen flow and washed with hot distilled water to remove remaining chemical and filtered. The washing and filtration steps were repeated until the filtrate became neutral. The washed activated carbon was dried at 105 °C for 24 h, ground to a particle size 150 μm and stored a plastic container for further use. The yield of activated carbon (yield = weight of BAC produced (g)/weight of dried bamboo (g)) was found to be 19.49.

Textural characterization of the prepared activated carbon was carried out by N_2 adsorption at 77 K using Autosorb I (Quantachrome Corporation, USA). The Brunauer–Emmett–Teller (BET) surface area and total pore volume of the prepared activated carbon were then determined. Scanning electron microscopy (SEM) analysis was carried out for the precursor and the prepared activated carbon to study their surface textures and the development of porosity. In addition, the surface functional groups of the prepared activated carbon were detected by Fourier transform infrared (FTIR) spectroscope (FTIR-2000, PerkinElmer). The spectra were recorded from 4000 to 400 cm^{-1}.

2.3. Adsorption studies

The batch sorption experiments were carried out in 250 mL Erlenmeyer flasks where 0.20 g of the BAC and 200 ml of the MG solutions (25–300 mg/L) were added without adjusting pH. The Erlenmeyer flasks were subsequently capped and agitated in an isothermal shaker at 120 rpm and 30 °C for 230 min to achieve equilibration. The concentration of the MG in the solution after equilibrium adsorption was measured by a double beam UV/vis spectrophotometer (Shimadzu, Model UV 1601, Japan) at 618 nm.

The amount of adsorption at equilibrium, q_e (mg/g), was calculated by:

$$q_e = \frac{(C_0 - C_e)V}{W} \quad (1)$$

where C_0 and C_e (mg/L) are the liquid-phase concentrations of dye at initial and equilibrium, respectively. V (L) is the volume of the solution and W (g) is the mass of dry adsorbent used.

To study the effect of solution pH, a sample of 0.20 g adsorbent was added to dye solution (200 ml, 50 mg/L) at constant temperature (30 °C). The experiments were carried out at pH 2–8. The Erlenmeyer flasks were subsequently capped and agitated in an isothermal shaker at 120 rpm and 30 °C for 230 min to achieve equilibration. The concentration of the MG in the solution after equilibrium adsorption was measured as above. The pH was adjusted by adding a few drops of diluted 0.1N NaOH or 0.1N HCl before each experiment. The pH was measured by using a pH meter (Ecoscan, EUTECH Instruments, Singapore).

Kinetic studies of adsorption were also carried out at various concentrations of the MG wherein the extent of adsorption was investigated as a function of time. The amount of adsorption at time t, q_t (mg/g), was calculated by:

$$q_t = \frac{(C_0 - C_t)V}{W} \quad (2)$$

3. Results and discussion

3.1. Characterization of activated carbon

Fig. 2 shows the SEM micrographs of BAC sample. It can be seen that the BAC surface exhibits a heterogeneous type pores. The multipoint BET surface area, total pore volume and average pore diameter were 1724 m^2/g, 1.071 cm^3/g and 2.485 nm, respectively. The BAC contained relatively large surface area and total pore volume compared to commercially available activated carbons. The high BET surface area and total pore volume

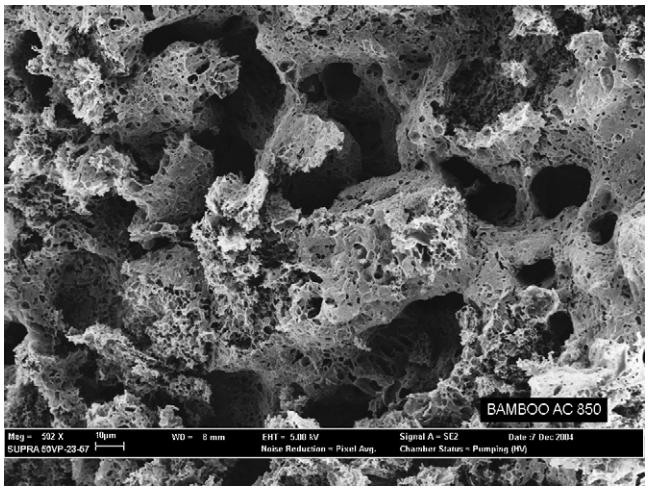

Fig. 2. SEM micrograph of BAC particle (magnification: 500).

of the prepared activated carbon was probably due to the activation process used, which involved both chemical and physical activating agents of K_2CO_3 and CO_2.

The FTIR spectra obtained (figure not shown) for the prepared activated carbon displayed the following bands (3853.03; 3736.46; 3672.52; 3650.09; 3630.45 cm^{-1} (OH stretch), 3567.95; 2374.35 cm^{-1} (NH stretch) and 1031.23 cm^{-1} (C–O stretch)).

3.2. Effect of initial concentrations and agitation time on dye adsorption

Fig. 3 shows the effect of initial MG concentration on the adsorption of the dye at pH 5, BAC dosage 0.20 g, and 30 °C. An increase in the initial MG concentration leads to a decrease in the MG removal. As the initial MG concentration increases from 25 to 300 mg/L the equilibrium removal of MG decreases from 98.60 to 84.45%. It is also noticed in Fig. 3 that large fractions of the total amount adsorbed of MG were removed in the initial rapid uptake phase. In the first 20 min, the fractions of total amounts adsorbed are about 95, 89, 92, 87, 77, 60 and 51

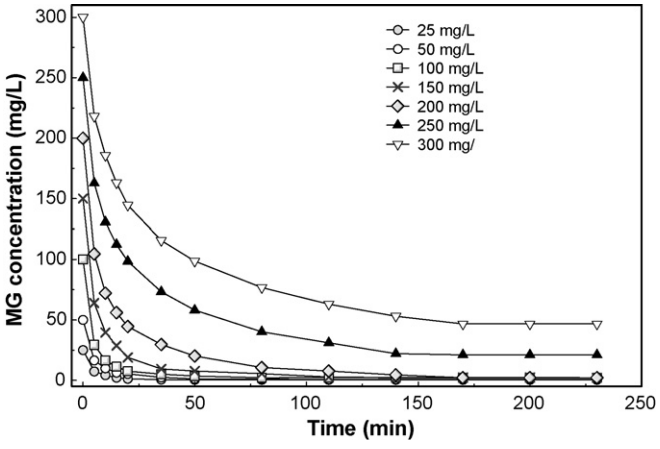

Fig. 3. Effect of initial concentration and contact time on MG adsorption (W = 0.20 g; temperature = 30 °C.).

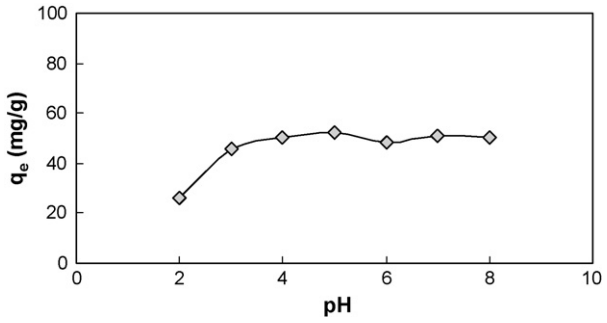

Fig. 4. Effect of pH on equilibrium uptake of MG (W = 0.20 g; V = 0.20 L; C_0 = 50 mg/L).

for initial MG concentrations 25, 50, 100, 150, 200, 250 and 300, respectively. This is due to the high concentration gradient in the beginning of adsorption which represents a high driving force for the transfer of MG from solution to the surface adsorbent. It is also clear from Fig. 3 that the contact time needed for MG solutions with initial concentrations of 25–50 mg/L to reach equilibrium was less than 50 min. For MG solutions with initial concentrations of 100–300 mg/L, the equilibrium time ranged between 80 and 170 min was required. However, the experimental data were measured at 230 min to make sure that full equilibrium was attained.

3.3. Effect of solution pH on dye adsorption

To study the effect of solution pH on MG adsorption, the experiment was conducted at initial concentration of 50 mg/L, 0.20 mg adsorbent at 30 °C. The effect of pH was studied in the range pH 2–8. The result is shown in Fig. 4. The amount of dye adsorbed at equilibrium, q_e increases from 26.25 to 50.11 with increase in pH from 2 to 8. The maximum q_e was observed at pH 4 and beyond that pH it attains almost constant value. Since no significant change in the adsorbed amount of dye was observed after pH 5, it was suggested that the increase in adsorption depended on the properties of the adsorbent surface and the dye structure. The behavior clearly indicates the protonation of MG in acidic medium and with the rise in pH the dye becomes more and more de-protonated. In lower pH range, the low adsorption of dye also exhibits possibility of development of positive charge at activated carbon surface, which inhibits the adsorption of dye over it [25]. However, in the basic medium the formation of electric double layer changes its polarity and consequently the dye uptake increases. A similar result was reported for adsorption of malachite green onto activated carbon prepared from Tunçbilek lignite [26].

3.4. Equilibrium isotherms

The thermodynamic assumptions of adsorption isotherms and their estimated parameters provide insight into both the properties of the surface and also the mechanism of adsorption. In this study, two isotherms were used for describing the experimental results, namely the Freundlich isotherm and the Langmuir isotherm.

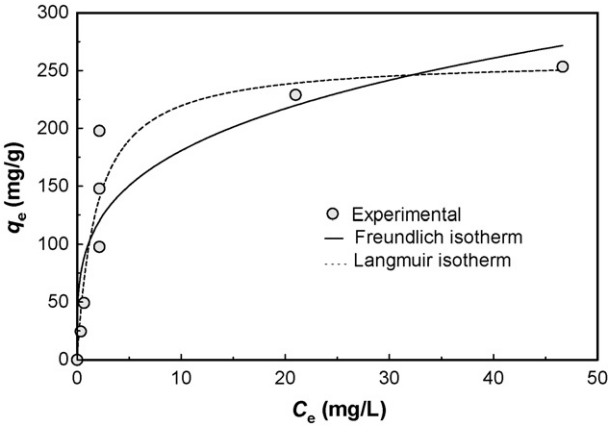

Fig. 5. Isotherm plots for MG adsorption on BAC at 30 °C.

The Freundlich isotherm is suitable for non-ideal adsorption on heterogeneous surfaces. The heterogeneity is caused by the presence of different functional groups on the surface, and several adsorbent–adsorbate interactions. The Freundlich isotherm is expressed by the following empirical equation [27]:

$$q_e = K_F C_e^{1/n} \quad (3)$$

where K_F (mg/g) (L/mg)$^{1/n}$ is the Freundlich adsorption constant and $1/n$ is a measure of the adsorption intensity.

Langmuir isotherm is derived on the assumption of monolayer adsorption on a homogenous surface. It is expressed by [28]:

$$q_e = \frac{q_m K_a C_e}{1 + K_a C_e} \quad (4)$$

where C_e is the equilibrium concentration (mg/L), q_e is the amount of dye adsorbed (mg/g), q_m is q_e for complete monolayer adsorption capacity (mg/g), and K_a is the equilibrium adsorption constant (L/mg).

Fig. 5 shows the fitted equilibrium data to Freundlich and Langmuir isotherms. The fitting results, i.e. isotherm parameters and the coefficient of determination, R^2, are shown in Table 1. It can be seen that the fitting to Freundlich isotherm is poor in comparison to Langmuir isotherm. This is also confirmed by the relatively high value of R^2 in case of Langmuir (0.9766) compared to Freundlich (0.9275). So the Freundlich isotherm can be rejected for the system MG–BAC.

Table 2 lists the comparison of maximum monolayer adsorption capacity of various activated carbons derived from different precursors reported in the literature [29–34] for the adsorption of MG. It can be concluded that the activated carbon prepared in this work has very large adsorption capacity.

Table 1
Isotherm constants for MG adsorption on BAC at 30 °C

Langmuir isotherm			Freundlich isotherm		
q_m (mg/g)	K_a (L/mg)	R^2	K_f	n	R^2
263.58	0.3864	0.9766	80.74	3.18	0.9275

Table 2
Comparison of adsorption capacities of various activated carbons for MG

Adsorbent	q_m (mg/g)	T (°C)	Reference
Bamboo-based activated carbon	263.58	30	This work
Cyclodextrin-based material	91.9	25	[29]
Groundnut shell-based powdered activated carbon (GSPAC)	222.22	30 ± 1	[30]
Commercial powder activated carbon (CPAC)	222.22	30 ± 1	[30]
Activated carbon prepared waste apricot	116.27	30	[31]
Activated carbons commercial grade (ACC)	8.27	30 ± 1	[32]
Activated carbons laboratory grade (ACL)	42.18	30 ± 1	[32]
Arundo donax root carbon (ADRC)	8.69	30	[33]
Lignite activated carbon	149	25	[34]
Oil palm trunk fibre	149.35	30	[35]
Bentonite clay	7.72	35	[36]
Chitosan bead	93.55	30	[37]

3.5. Kinetic study

The modeling of the kinetics of adsorption of MG on BAC was investigated by three common models, namely, the Lagergren pseudo-first-order model (Eq. (5)) [38], Ho's pseudo-second-order model (Eq. (6)) [39], and the Elovich model (Eq. (7)) [40].

$$q = q_e(1 - e^{-k_1 t}) \quad (5)$$

$$q = \frac{q_e^2 k_2 t}{1 + q_e k_2 t} \quad (6)$$

$$q = \frac{1}{\beta} \ln(1 + \alpha\beta t) \quad (7)$$

where q_e is the amount of MG adsorbed at equilibrium (mg/g), q is the amount of MG adsorbed at time t (mg/g), k_1 is the rate constant of pseudo-first-order adsorption (min^{-1}), k_2 is the rate constant of pseudo-second-order adsorption (g/mg min), α is the initial adsorption rate (mg/g min), and β is the desorption constant (g/mg).

The fittings of the experimental kinetic results to the three models are shown in Figs. 6–8, and the estimated parameters values are presented in Table 3. It can be seen from the R^2 values that the pseudo-second-order model gives the best fit (R^2: 0.9952–0.9993) but its predicted q_e values are overestimated as compared to the experimentally observed values (2.3–5.6% deviation), especially at high MG concentrations. However, q_e values estimated from the pseudo-second-order model are an extrapolation outside the time period that was experimentally investigated, the fact still remains that the model accurately predicts the adsorption kinetics throughout the period of experiments. Therefore, the pseudo-second-order model could be used for the prediction of the kinetics of adsorption of MG on BAC. As for the other two models, it is not clear that there is a second best; Lagergren's model performs reasonably well at low MG concentration and the goodness of fit deteriorates

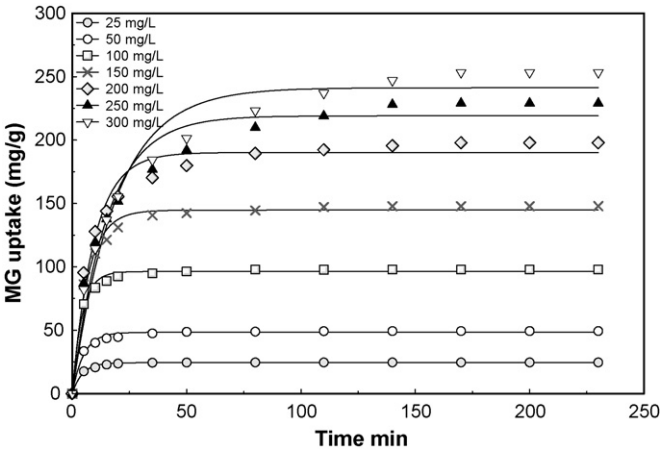

Fig. 6. The fitting of Lagergren's model for MG on BAC for different initial concentrations at 30 °C.

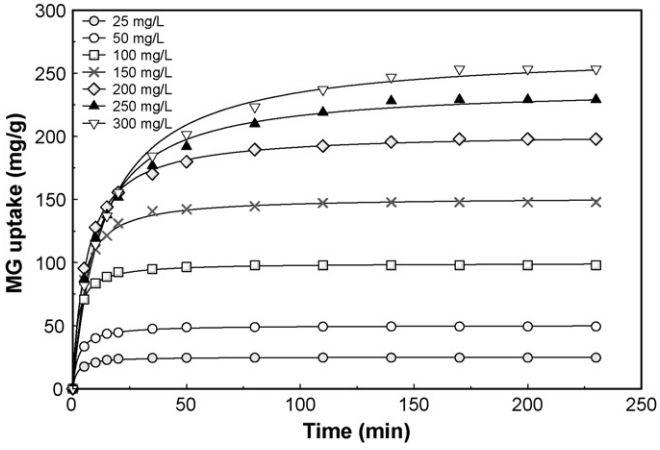

Fig. 7. The fitting of pseudo-second-order model for MG on BAC for different initial concentrations at 30 °C.

at higher concentrations, while Elovich model has the poorest fitting at low concentrations but improves at higher MG concentrations.

The initial adsorption rates can be calculated from the pseudo-second-order model by the following equation:

$$h_{o,2} = k_2 q_e^2 \quad (8)$$

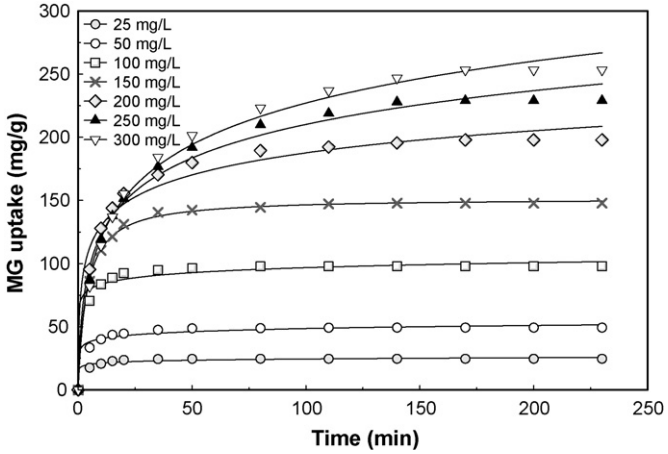

Fig. 8. The fitting of Elovich model for MG on BAC for different initial concentrations at 30 °C.

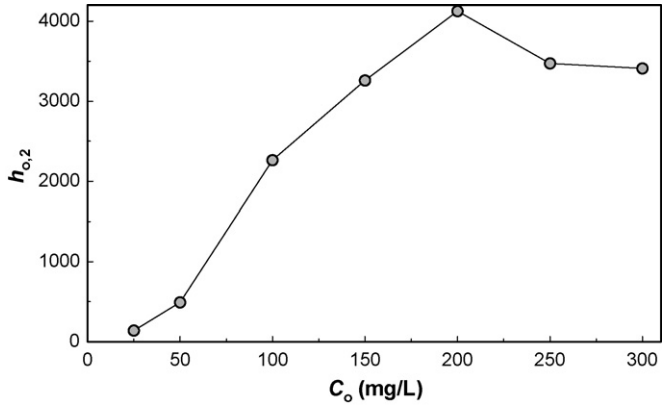

Fig. 9. The variation of the initial rate of adsorption with the initial MG concentration.

and the results are plotted in Fig. 9. It was found that the initial rate of adsorption increases with increasing the initial MG concentration, reaches its maximum value when $C_o = 200$ mg/L, then decreases slightly at higher initial MG concentrations. The initial increase in $h_{o,2}$ is probably caused by the increase in driving force for mass transfer with increasing concentration, then at still higher concentrations, the effect of MG dimerization becomes apparent [41,42] making the diffusion of large dimers more difficult in small pores.

Table 3
Kinetic models parameters for the adsorption of MG on BAC at 30 °C and different initial MG concentrations (C_o: mg/L; q_e: mg/g; k_1: min^{-1}; k_2: g/mg min, α: mg/g min and β: g/mg)

Pseudo-first-order					Pseudo-second-order			Elovich equation		
C_o	q_{exp}	q_e	k_1	R^2	q_e	k_2	R^2	α	β	R^2
25	24.66	24.43	0.228	0.9938	25.24	0.0202	0.9963	451886	0.706	0.9713
50	49.34	48.39	0.201	0.9863	50.33	0.00809	0.9992	37540	0.286	0.9773
100	97.87	96.29	0.236	0.9912	99.61	0.00519	0.9992	1283869	0.175	0.9800
150	147.86	144.71	0.149	0.9872	151.84	0.00180	0.9987	151.84	0.00180	0.9987
200	197.86	190.17	0.105	0.9735	202.87	0.000830	0.9993	433.72	0.0397	0.9796
250	229.02	219.12	0.0662	0.9629	239.46	0.000393	0.9952	89.04	0.0259	0.9897
300	253.63	241.28	0.0530	0.9666	267.96	0.000265	0.9955	53.68	0.0208	0.9927

3.6. Mechanism of adsorption

For practical applications of adsorption such as process design and control, it is important to understand the dynamic behavior of the system. At the present time, Webber's pore-diffusion model [43] and Boyd's equation [44] are the two most widely used models for studying the mechanism of adsorption.

The model of Boyd was originally proposed for intraparticle diffusion in ion exchangers and is expressed as:

$$F = 1 - \left(\frac{6}{\pi^2}\right)\sum_{n=1}^{\infty}\left(\frac{1}{n^2}\right)\exp(-n^2 Bt) \quad (9)$$

where F is the fractional attainment of equilibrium, at different times, t, and Bt is a function of F

$$F = \frac{q_t}{q_e} \quad (10)$$

where q_t and q_e are the dye uptake (mg/g) at time t and at equilibrium, respectively.

From Eq. (9), it is not possible to estimate directly the values of B for each fraction adsorbed. By applying the Fourier transform and then integration, Reichenberg [45] managed to obtain the following approximations:

$$\text{for } F \text{ values} > 0.85, \quad Bt = -0.4977 - \ln(1 - F) \quad (11)$$

and for F values < 0.85,

$$Bt = \left(\sqrt{\pi} - \sqrt{\pi - \left(\frac{\pi^2 F}{3}\right)}\right)^2 \quad (12)$$

B, can be used to calculate the effective diffusion coefficient, D_i (cm^2/s) from the equation:

$$B = \frac{\pi^2 D_i}{r^2} \quad (13)$$

where r is the radius of the adsorbent particle assuming spherical shape.

Eqs. (10)–(13) can be used in predicting the mechanistic steps involved in the adsorption process, i.e. whether the rate of removal of the dye takes place via particle diffusion or film diffusion mechanism. This is done by plotting Bt against time, if the plot is linear and passes through the origin then pore diffusion controls the rate of mass transfer. If the plot is nonlinear or linear but does not pass through the origin, then it is concluded that film-diffusion or chemical reaction control the adsorption rate.

On the other hand, Webber's pore-diffusion model is another single-resistance model that was derived from Fick's second law of diffusion. This model assumes that:

(i) the external resistance to mass transfer is only significant for a very short period at the beginning of diffusion;
(ii) the direction of diffusion is radial and the concentration;
(iii) the pore diffusivity is constant and does not change with neither time.

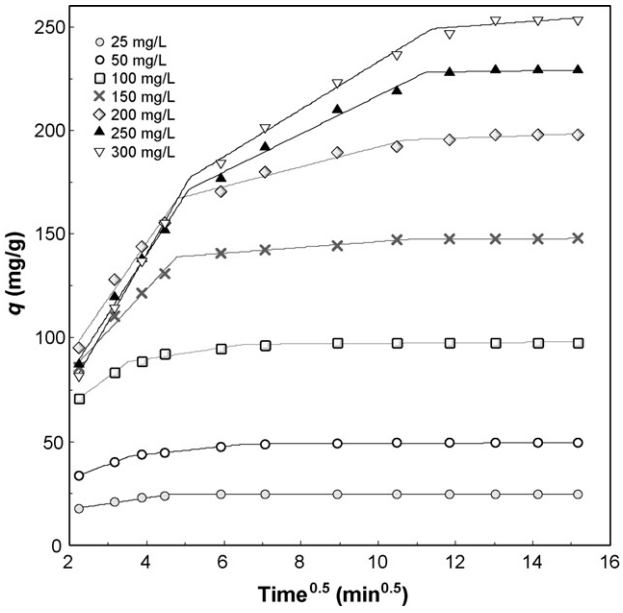

Fig. 10. Intraparticle diffusion plot for the adsorption at 30 °C and different initial MG concentrations.

The pore diffusion parameter, k_i (mg/g $min^{0.5}$) is defined by:

$$q = k_i t^{0.5} + c \quad (14)$$

where q is the amount adsorbed (mg/g) at time t.

It can be seen from Eq. (14) that if pore diffusion is the rate limiting step, then a plot of q against $t^{0.5}$ must give a straight line with a slope that equals k_i and the intercept value, c, represents the resistance to mass transfer in the external liquid film.

Fig. 10 shows the pore diffusion plot of MG adsorption on BAC at 30 °C. It is clear that the plots are multilinear, containing at least three linear segments. The software package NCSS [46] was used to fit the data to the model by the method of piecewise linear regression, the regression results are presented in Table 4. For all the multilinear plots in Fig. 10, the regression estimates of the first linear segments had intercept values different from zero, suggesting that pore diffusion is not the step controlling the overall rate of mass transfer at beginning of batch adsorption. Film-diffusion control may have taken place and ended in the early stages of adsorption (from 0 to 5 min), or maybe it is still controlling the rate of mass transfer in the time period of the first

Table 4
Diffusion coefficients for adsorption of MG on BAC at 30 °C and different initial concentrations (C_o: mg/L; k_i: mg/g $min^{0.5}$; diffusion period: min)

C_o	$k_{i,1}$	Intercept	$k_{i,2}$	First pore diffusion period[a]	Second pore diffusion period[b]
25	3.34	10.53	0.51	5.0–16.6	16.6–39.9
50	7.06	17.77	1.92	5.0–12.8	12.8–43.5
100	13.90	39.60	2.76	5.0–12.5	12.5–43.0
150	19.93	43.74	1.40	5.0–22.9	22.9–121.0
200	26.82	38.51	4.79	5.0–23.0	23.0–114.5
250	28.73	25.26	9.21	5.0–25.9	25.9–125.9
300	32.86	9.28	11.47	5.0–26.0	26.0–129.7

[a] Estimated from the first linear segment in the pore-diffusion model.
[b] Estimated from the second linear segment in the pore-diffusion model.

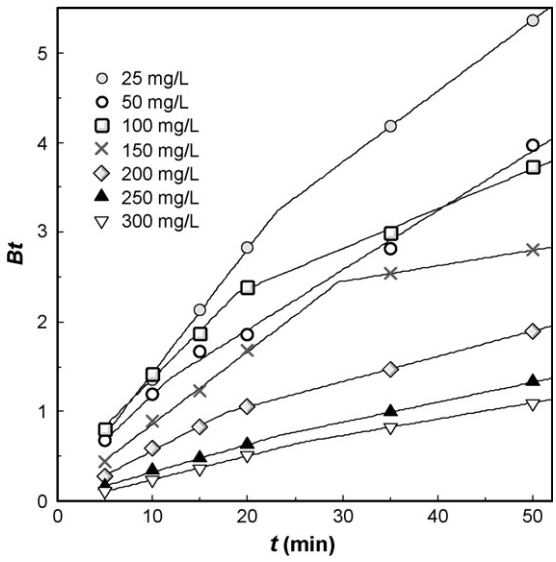

Fig. 11. Boyd plots for MG adsorption on BAC at 30 °C and different initial MG concentrations.

linear segment. A conclusion can be reached from the analysis of data by Boyd's model.

Fig. 11 shows the Boyd plots for the first 50 min of MG adsorption on BAC at 30 °C. The plots are linear in the initial period of adsorption and all their slopes are not significantly different from zero, indicating that pore diffusion is the rate limiting process, and thus corroborating the conclusion that pore diffusion is the rate limiting step throughout the whole adsorption period studied (from 5 min until equilibrium). For adsorption time shorter than 5 min, film-diffusion or chemical-reaction maybe controlling the overall rate of adsorption. The absence of experimental data in the period 0–5 min does not allow the determination of the rate controlling step in this period.

The presence of two pore diffusion periods in Fig. 10 indicates the presence of two pore diffusion parameters, $k_{i,1}$ and $k_{i,2}$ as shown in Table 4. The rate parameters $k_{i,1}$ and $k_{i,2}$ represent the diffusion in of MG in pores that have two distinct sizes (macropores and mesopores) [47]. Therefore, the decrease in value of k for macropore to mesopore diffusion is a direct consequence of the relative free path for diffusion available in each pore size. As pore size decreases, the path available for diffusion becomes smaller, which leads to a decrease in the rate of diffusion. It is also observed in Table 4 that an increase in the initial MG concentration increases the pore diffusion rate parameters. This is due to the increase in the bulk liquid dye concentration which increases the driving force of dye diffusion.

4. Conclusions

The results of this work can be summarized as follows:

1. The present study shows that activated carbon prepared from bamboo can be used as an adsorbent for the removal of malachite green dye from aqueous solutions.
2. The amount of dye adsorbed was found to vary with initial of malachite green concentration and contact time. Langmuir isotherm was found to have the best fit to the experimental data, suggesting monolayer adsorption on a homogenous surface.
3. The adsorption kinetics can be predicted by the pseudo-second-order model.
4. The overall rate of dye uptake was found to be controlled by pore diffusion throughout the entire adsorption period studied (from 5 min until equilibrium). For adsorption time shorter than 5 min, film-diffusion or chemical-reaction maybe controlling the overall rate of adsorption.

Acknowledgements

The authors acknowledge the research grant provided by the Universiti Sains Malaysia under the Research University (RU) Scheme (Project No. 1001/PJKIMIA/814005). The authors thank Ms. I.A.W. Tan for her assistance in FTIR analysis.

References

[1] G. Mishra, M. Tripathy, A critical review of the treatment for decolourization of textile effluent, Colourage 40 (1993) 35–38.
[2] Y. Fu, T. Viraraghavan, Fungal decolourization of wastewaters: a review, Bioresour. Technol. 79 (2001) 251–262.
[3] E.A. Clarke, R. Anliker, Organic dyes and pigments, in: Handbook of Environmental Chemistry, Anthropogenic Compounds, Part A, vol. 3, Springer Verlag, New York, 1980, pp. 181–215.
[4] I.M. Banat, P. Nigam, D. Singh, R. Marchant, Microbial decolourization of textile-dye containing effluents: a review, Bioresour. Technol. 58 (1996) 217–227.
[5] A.K. Mittal, S.K. Gupta, Biosorption of cationic dyes by dead macro fungus *Fomitopsis carnea*: batch studies, Water Sci. Technol. 34 (1996) 157–181.
[6] H.C. Chu, K.M. Chen, Reuse of activated sludge biomass. I. Removal of basic dyes from wastewater by biomass, Process. Biochem. 37 (2002) 595–600.
[7] Y. Fu, T. Viraraghavan, Removal of Congo Red from an aqueous solution by fungus *Aspergillus niger*, Adv. Environ. Res. 7 (2002) 239–247.
[8] H. Zollinger, Azo Dyes and Pigments. Colour Chemistry—Synthesis, Properties and Applications of Organic Dyes and Pigments, VCH, New York, 1987, pp. 92–100.
[9] T. Robinson, G. Mcmullan, R. Marchant, P. Nigam, Remediation of dyes in textile effluent: a critical review on current treatment technologies with a proposed alternative, Bioresour. Technol. 77 (2001) 247–255.
[10] S. Srivastava, R. Sinha, D. Roy, Toxicological effects of malachite green, Aquat. Toxicol. 66 (2004) 319–329.
[11] J.C. Sandra, R.B. Lonnie, F.K. Donna, R.D. Daniel, T. Louis, A.B. Frederick, Toxicity and metabolism of malachite green and leucomalachite green during short-term feeding to Fischer 344 rats and B6C3F1 mice, Chem.-Biol. Interact. 122 (1999) 153–170.
[12] E. Forgacs, T. Cserháti, G. Oros, Removal of synthetic dyes from wastewaters: a review, Environ. Int. 30 (2004) 953–971.
[13] K. Wu, Y. Xie, J. Zhao, H. Hidaka, Photo-Fenton degradation of a dye under visible light Irradiation, J. Mol. Catal. A: Chem. 144 (1999) 77–84.
[14] C. Hachem, F. Bocquillon, O. Zahraa, M. Bouchy, Decolourization of textile industry wastewater by the photocatalytic degradation process, Dyes Pigments 49 (2001) 117–125.
[15] H. Kominami, H. Kumamoto, Y. Kera, B. Ohtani, Photocatalytic decolorization and mineralization of malachite green in an aqueous suspension of titanium(IV) oxide nano-particles under aerated conditions: correlation between some physical properties and their photocatalytic activity, J. Photochem. Photobiol. A Chem. 160 (2003) 99–104.
[16] G. Crini, Non-conventional low-cost adsorbents for dye removal: a review, Bioresour. Technol. 97 (2006) 1061–1085.

[17] I.A.W. Tan, B.H. Hameed, A.L. Ahmad, Equilibrium and kinetic studies on basic dye adsorption by oil palm fibre activated carbon, Chem. Eng. J. 127 (2007) 111–119.
[18] B.H. Hameed, A.L. Ahmad, K.N.A. Latiff, Adsorption of basic dye (methylene blue) onto activated carbon prepared from rattan sawdust, Dyes Pigments 75 (2007) 143–149.
[19] I.A.W. Tan, A.L. Ahmad, B.H. Hameed, Optimization of preparation conditions for activated carbons from coconut husk using response surface methodology, Chem. Eng. J. 137 (2008) 462–470.
[20] B.H. Hameed, F.B.M. Daud, Adsorption studies of basic dye on activated carbon derived from agricultural waste: *Hevea brasiliensis* seed coat, Chem. Eng. J. 139 (2008) 48–55.
[21] B.H. Hameed, A.T.M. Din, A.L. Ahmad, Adsorption of methylene blue onto bamboo-based activated carbon: kinetics and equilibrium studies, J. Hazard. Mater. 141 (2007) 819–825.
[22] D. Adinata, W.M.A. Wan Daud, M.K. Aroua, Preparation and characterization of activated carbon from palm shell by chemical activation with K_2CO_3, Bioresour. Technol. 98 (2007) 145–149.
[23] A.P. Carvalho, M. Gomes, A.S. Mestre, J. Pires, M. Brotas de Carvalho, Activated carbons from cork waste by chemical activation with K_2CO_3. Application to adsorption of natural gas components, Carbon 42 (2004) 667–691.
[24] J. Hayashi, T. Horikawa, K. Muroyama, V.G. Gomes, Activated carbon from chickpea husk by chemical activation with K_2CO_3: preparation and characterization, Microporous Mesoporous Mater. 55 (2002) 63–68.
[25] V.K. Gupta, A. Mittal, L. Krishnan, V. Gajbe, Adsorption kinetics and column operations for the removal and recovery of malachite green from wastewater using bottom ash, Sep. Purif. Technol. 40 (2004) 87–96.
[26] Y. Önal, C. Akmil-Başar, D. Eren, Ç. Sarıcı-Özdemir, T. Depci, Adsorption kinetics of malachite green onto activated carbon prepared from Tunçbilek lignite, J. Hazard. Mater. B128 (2006) 150–157.
[27] H.M.F. Freundlich, Over the adsorption in solution, J. Phys. Chem. 57 (1906) 385–470.
[28] I. Langmuir, The constitution and fundamental properties of solids and liquids, J. Am. Chem. Soc. 38 (11) (1916) 2221–2295.
[29] G. Crini, H.N. Peindy, F. Gimbert, C. Robert, Removal of C.I. Basic Green 4 (malachite green) from aqueous solutions by adsorption using cyclodextrin-based adsorbent: kinetic and equilibrium studies, Sep. Purif. Technol. 53 (2007) 97–110.
[30] R. Malik, D.S. Ramteke, S.R. Wate, Adsorption of malachite green on groundnut shell waste based powdered activated carbon, Waste Manage. 27 (2007) 1129–1138.
[31] C.A. Başar, Applicability of the various adsorption models of three dyes adsorption onto activated carbon prepared waste apricot, J. Hazard. Mater. B135 (2006) 232–241.
[32] I.D. Mall, V.C. Srivastava, N.K. Agarwal, I.M. Mishra, Adsorptive removal of malachite green dye from aqueous solution by bagasse fly ash and activated carbon-kinetic study and equilibrium isotherm analyses, Colloids Surf. A: Physicochem. Eng. Aspects 264 (2005) 17–28.
[33] J. Zhang, Y. Li, C. Zhang, Y. Jing, Adsorption of malachite green from aqueous solution onto carbon prepared from *Arundo donax* root, J. Hazard. Mater. 150 (2008) 774–782.
[34] Y. Önal, C. Akmil-Başar, Ç. Sarıcı-Özdemir, Investigation kinetics mechanisms of adsorption malachite green onto activated carbon, J. Hazard. Mater. 146 (2007) 194–203.
[35] B.H. Hameed, M.I. El-Khaiary, Batch removal of malachite green from aqueous solutions by adsorption on oil palm trunk fibre: equilibrium isotherms and kinetic studies, J. Hazard. Mater. 154 (2008) 237–244.
[36] S.S. Tahir, N. Rauf, Removal of a cationic dye from aqueous solutions by 491 adsorption onto bentonite clay, Chemosphere 63 (2006) 1842–1848.
[37] Z. Bekçi, C. Özveri, Y. Seki, K. Yurdakoç, Sorption of malachite green on chitosan bead, J. Hazard. Mater. 154 (2008) 254–261.
[38] S. Lagergren, Zur theorie der sogenannten adsorption geloster stoffe. 591. Kungliga Svenska Vetenskapsakademiens, Handlingar 24 (4) (1898) 1–39.
[39] Y.S. Ho, Adsorption of heavy metals from waste streams by peat, Ph.D. Thesis, University of Birmingham, Birmingham, UK, 1995.
[40] C. Aharoni, D.L. Sparks, S. Levinson, I. Ravina, Kinetics of soil chemical reactions: relationships between empirical equations and diffusion models, Soil Sci. Soc. Am. J. 55 (1991) 1307–1312.
[41] N. Strataki, V. Bekiari, P. Lianos, Study of the conditions affecting dye adsorption on titania films and of their effect on dye photodegradation rates, J. Hazard. Mater. 146 (2007) 514–519.
[42] R.N. Muir, A.J. Alexander, Structure of monolayer dye films studied by Brewster angle cavity ring down spectroscopy, Phys. Chem. Chem. Phys. 5 (2003) 1279–1283.
[43] W.J. Weber Jr., J.C. Morris, Kinetics of adsorption on carbon from solution, J. Sanitary Eng. Div. Proceed. Am. Soc. Civil Eng. 89 (1963) 31–59.
[44] G.E. Boyd, A.W. Adamson, L.S. Myers Jr., The exchange adsorption of ions from aqueous solutions by organic zeolites. II. Kinetics, J. Am. Chem. Soc. 69 (1947) 2836–2848.
[45] D. Reichenberg, Properties of ion exchange resins in relation to their structure. III. Kinetics of exchange, J. Am. Chem. Soc. 75 (1953) 589–598.
[46] J. Hintze, NCSS, PASS and GESS, NCSS, Kaysville, Utah, 2006.
[47] S.J. Allen, G. McKay, K.Y.H. Khader, Intraparticle diffusion of a basic dye during adsorption onto sphagnum peat, Environ. Pollut. 56 (1989) 39–50.